Theoretical studies of hydrogen bonding in liquid water and dilute aqueous solutions

Mihaly Mezei and David L. Beveridge

Chemistry Department, Hunter College of the City University of New York, New York, New York 10021
(Received 2 May 1980; accepted 13 May 1980)

Monte Carlo computer simulations of liquid water and dilute aqueous solutions are analyzed in terms of the nature and extent of intermolecular hydrogen bonding. A geometric definition of the hydrogen bond is used. Calculations on liquid water at 25 °C, 37 °C, and 50 °C, were carried out based on the quantum mechanical MCY potential of Matsuoka, Clementi, and Yoshimine and at 10 °C based on the empirical ST2 potential. The effect of a dissolved solute on aqueous hydrogen bonding was studied for dilute aqueous solutions of Li^+, Na^+, K^+, F^-, Cl^-, and CH_4. The nature of the hydrogen bonding was characterized with quasicomponent distribution functions defined as a function of the intermolecular coordinates relevant to hydrogen bonding. The extent of the hydrogen bonding is described using a network analysis approach developed by Geiger, Stillinger, and Rahman. The results on the quasicomponent distribution functions show that the average hydrogen bond angle deviates with 10°–25° from a linear form, quite independently of the potential function. The decrease in icelike character in liquid water as the temperature is increased is quantified. The structuration effects in solvent water for dilute aqueous solution of ionic and hydrophobic solutes are computed, and interpreted in terms of the Frank and Wen *A*, *B* and *C* regions of solvent. There is increased structure in the *A* region of both the ionic and apolar solutes, electrostrictive for the former and clathratelike for the latter. The *B* region is destructured in ionic solutions and shows increased icelike structural character in the solution of an apolar solute. The network analysis showed the existence of large space-filling hydrogen bonded networks. The occurrence of monomers was found to be negligibly small. These findings are in quantitative agreement with the analysis of molecular dynamics results by Geiger *et al.*, based on an energetic hydrogen bond definition. Furthermore, the parameters of the distributions of the hydrogen bonded networks were found to be remarkably invariant to small change in the temperature, introduction of a solute and the change of the potential function. The average cluster size and related parameters are quite sensitive to the number of molecules considered. Overall, the analysis supports the validity of viewing liquid water in terms of a Pople continuum and Sceats–Rice random network model of water molecules interacting mainly via bent hydrogen bonds.

I. INTRODUCTION

In a series of recent papers[1–6] we reported on statistical thermodynamic Monte Carlo computer simulations of liquid water and dilute aqueous solutions of prototype hydrophobic and ionic solutes. The agreement between calculated and available observed thermodynamic indices was sufficiently close to expect that a reasonable view of the structure of each system could be extracted from the results. In these studies, the composition of the systems was described in terms of structural and energetic quasicomponent distribution functions (QCDF),[7] principally the mole fractions $x_C(K)$ for coordination number K, $x_B(\nu)$ for binding energy ν, and to a lesser extent $x_D(\theta)$ for dipole–dipole angle θ and $x_D(\epsilon)$ for pair energies ϵ. However, the principal compositional characteristic of water and aqueous solutions is intermolecular hydrogen bonding (H bonding), dealt with only implicitly in our QCDF analyses to date. We have recently formulated QCDF's specifically for H-bond indices and carried out analyses of the nature of H bonding in Monte Carlo computer simulated liquid water and aqueous solutions. In a further elaboration of the analyses, the extent of H bonding is developed in terms of a statistical "network analysis"[8] of each case. The results are collected and described herein.

The background for this study is given in Sec. II. The theory and methodology of the analysis is given in Sec. III, followed in Sec. IV by a description of the calculations. The results are presented in Sec. V, followed in Sec. VI by summary and conclusions.

II. BACKGROUND

Intermolecular H bonding is qualitatively well understood to be the preferential stabilizing interaction of an electropositive hydrogen atom on one molecule with an electronegative atom such as oxygen on another molecule. The essential electrostatic nature of this interaction has been revealed by detailed analyses of quantum mechanical calculations of H-bonded dimers.[9–13] In order to develop a H-bond analysis of a molecular liquid, it is necessary to postulate a quantitative definition of a H bond. This definition is used to ascertain whether or not any two molecules are H bonded, and thus incorporated into H-bond indices defined on the statistical state of the molecular liquid at a specified temperature.

There are two possible approaches to quantitatively defining a H bond: energetic and geometric. In the energetic approach, two molecules with interaction energy below some threshold energy V_{HB} are taken to be H bonded. This alternative has been generally adopted in H-bond analyses of the molecular dynamics studies on liquid water by Rahman and Stillinger[14] based on the empirical ST2 intermolecular potential function.[15] This approach is particularly applicable in the case of water, where it is reasonable to assume that H bonding is the predominant energy-stabilizing interaction. Rahman and Stillinger's analyses were carried out as a function of V_{HB} over the reasonable range of assumed values. The dispersion of H-bond energies in liquid water were found to be smooth and unimodal in all cases studied.

 0021-9606/81/010622-11$01.00

The analysis of Monte Carlo computations based on the quantum mechanical MCY[13] potential by Owicki and Scheraga[16] and by Swaminathan and Beveridge[2] in terms of $x_B(\nu)$ and related quantities independently supported the unimodal nature of the energetic environments of water molecules in the liquid. Jorgensen recently applied an energetic definition of H bonding in an analysis of liquid water based on a quantum mechanical STO-3G intermolecular potential function.[17-19] Collectively, the computer simulation results to date are generally consistent with the energetic continuum model of liquid water introduced earlier by Pople,[20] where the liquid is viewed in terms of a spatially homogeneous distribution of progressively "bent" hydrogen-bonded species.

The geometric definition of H bond, the basis for the calculations described herein, is developed in terms of the internal coordinates of the dimeric species relevant to the intermolecular interactions. In the case of the water dimer the relevant coordinates are the interoxygen separation, hydrogen–oxygen–oxygen and lone pair–oxygen–oxygen bond angles and the hydrogen–oxygen–lone pair dihedral angle.[21] The H-bond analysis is based on the mole fraction of species in the fluid developed as a function of each of these geometric parameters over a reasonable range of values. Jorgensen in the paper cited above also reported results of H-bond distribution on angular coordinates[19] with a different H-bond angle definition. His average H-bond angle value was in close agreement with the value assumed by Pople in 1951.[20] The geometric approach restricts the definition to discretely H-bonded species and can be generalized straightforwardly to systems other than water and water-like species. The structure information emergent from this approach is directly related to parameters in the original Pople model for liquid water and the very recent extension of the idea by Rice and Sceats in terms of the random network model.[21,22]

The energetic and geometric definitions of hydrogen bonding must, of course, be closely related, since interaction energy is an explicit function of the geometric parameters. Considered separately, the energetic criterion has the advantage of being easily transferred to various types of H-bonding situations. It disadvantageously depends on the potential function assumed in the simulation and thus a comparison of H bonding in simulations based on different reasonable intermolecular potential functions may not be straightforward. Furthermore, as the results of Jorgensen on liquid HF revealed,[23] it can admit relative orientations which are contrary to our qualitative notion of H bonding. The geometric definition is independent of the intermolecular potentials assumed, but with it a comparison of H bonding involving different types of acceptor atoms is not necessarily straightforward. Although we do not pursue this point herein, we note that the energetic and geometric criteria could be used together in conjunction with joint quasicomponent distribution functions to analyze the structure of a H-bonded fluid.[7] In any case, with a quantitative definition of intermolecular H bonding at hand, the nature of H bonding in a liquid can be displayed using the H-bonding QCDF.

A full H-bonding analysis of a molecular fluid should deal not only with the nature of H bonding in the system but also the extent of H bonding. A general approach to this aspect of the problem has been developed by Geiger, Stillinger, and Rahman in terms of "network analysis."[8] In network analysis, the number and size of H-bonded clusters is determined for several N-particle configurations of the system and the corresponding configurationally averaged quantities and statistical distributions are computed. The analysis of molecular dynamics results on liquid water using this approach revealed a percolation threshold for the liquid well below the minimum reasonable value for V_{HB}, thus supporting the description of liquid water in terms of a large space filling random network of H-bonded molecules.

Both temperature changes and the introduction of a solute perturb the water structure and alter the nature and extent of H bonding. These solute effects have been described by solution chemists in terms of "structural temperature," i.e., the temperature at which the value of a property of liquid water is equal to that of the solution at 25 °C. The structural chemistry of solutions is also described in terms of "structure making" and "structure breaking," empirically defined indices of the effect of solute perturbations on solvent water structure. These all have been generally useful approaches to systematizing results on very complex physicochemical systems. Nevertheless, many ambiguities arise in practical applications.[24]

To consider these effects further it is convenient following Frank and Wen[25] to subdivide the solvent into regions labeled A, B, and C. The A region is the immediate vicinity of the solute, and can be provisionally identified with the first solvation shell. Region C is bulk water. The B region structurally interfaces regions A and C. The net structuration of a solution as manifested in observed physical properties is the resultant of A-region and B-region solvent perturbations.

It is important to note that the structuration of solvent water may occur in more than one way. The structure could assume more icelike character, i.e., show an increase in the mole fraction of four-coordinate species and show an increased preference for stronger, more linear H bonds. Alternatively, solutes with strong solute–water binding tendencies such as ions could cause completely new highly ordered structures to be introduced into the liquid. Structurally more complex solutes may show a combination of these effects. Any one or combination of these effects may of physical properties diagnostic of "structure."

In principle, the H-bond QCDF's and network analysis as described above for liquid water could be used for the analysis of computer simulation results on aqueous solutions, providing a formal basis for critical analysis of empirical indices of structure and information about the various forms of solvent water structure at the molecular level. Here it is necessary to have simulations on liquid water and aqueous solutions carried out at commensurate and consistent levels of approximation, and to calculate difference H-bond QCDF's and related structural indices for the A and B regions. We have recently

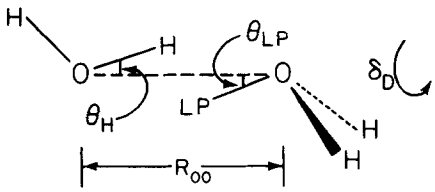

FIG. 1. The definition of the H-bond parameters.

carried out a number of studies in this vein whose results to date are described herein. The systems under considerations are liquid water at several ambient temperatures and dilute aqueous solutions of prototype ionic and hydrophobic solutes at 25 °C. The sensitivity of the results to the choice of water–water potential and the convergence characteristics of computer simulations are concomitantly explored.

III. THEORY

The four internal coordinates of the water dimer that are relevant for the description of H bonding are defined in Fig. 1.[21] Here R_{OO} is the interoxygen separation, the angle θ_H is the angle between the H–O and O–O bonds, and θ_{LP} is the angle between the LP–O and O–O bonds. The angle δ_D is the dihedral angle between the planes H–O–O and LP–O–O. In these definitions, LP is a suitably located "pseudoatom" on the water molecule, corresponding to the qualitative idea of tetrahedrally oriented lone-pair (LP) orbitals. For ST2 water the LP pseudoatoms were chosen to coincide with the negative charges on the water, while for the MCY water they were placed in such a way that the LP–O–LP triangle is of the same dimensions as the H–O–H triangle and oriented perpendicular to it. Note that the LP positions for the analysis are not related to any terms in the analytical MCY potential function. For each water, the atom/pseudoatom participating in a H bond with another water was taken as the atom on the donor water closest to the oxygen atom of the acceptor water.

A quantitative geometric definition of the H bond further requires the specification of cutoff values for each of these parameters. The strength assumed for the H bond can be modified by varying the cutoff values. Qualitative notions on the H bond place an upper bound on θ_H and θ_{LP} since it is natural to require that the atoms on one molecule proximal to the oxygen of the other molecule should be an H and an LP, respectively. The tetrahedral character of the interaction leads to a "minimal" definition of the H bond as

$$\begin{aligned} &R_{OO} \le R_{max} , \\ &\theta_H \le 70.53^\circ , \\ &\theta_{LP} \le 70.53^\circ , \\ &\delta_D \le 180.0^\circ . \end{aligned} \tag{1}$$

A natural choice for R_{max} is the cutoff value R_M for the previously determined coordination number distribution function, 3.3 Å.

The four parameters described above give rise to the following four H-bonding QCDF's:

$$x_H(u_h) = \int \sum_{i<j}^{N} \delta[u_h^{ij}(\mathbf{X}^N) - u_h] P(\mathbf{X}^N) C_{ij}(\mathbf{X}^N) d\mathbf{X}^N \times \left(\int \sum_{i<j}^{N} P(\mathbf{X}^N) C_{ij}(\mathbf{X}^N) d\mathbf{X}^N \right)^{-1} , \tag{2}$$

where the four possible choices of u_h are

$$u_1 = R_{OO} , \quad u_2 = \theta_H , \quad u_3 = \theta_{LP} , \quad u_4 = \delta_D . \tag{3}$$

Here $u_h^{ij}(\mathbf{X}^N)$ is the value of the parameter u_h for the pair (i,j), $\delta[\ ]$ is the Dirac delta. The quantity $C_{ij}(\mathbf{X}^N)$ is a counting function for the H bond: it equals to one if the pair (i,j) is H bonded and to zero otherwise. Joint QCDF's of the four parameters can be readily defined analogously to those for coordination number and binding energy reported earlier. Furthermore, in studying structural parameters in statistical mechanical context, it should be noted that there are both probabilistic and energetic factors to consider, and that the most favorable parameter value energetically may not be the most probable, particularly when it is associated with a relatively small region of configuration space. This circumstance is expressed quantitatively by a comparison of $x_H(u_h)$ and $x_H(u_h)/v(u_h)$, the latter quantity being normalized by the volume element of the configuration space with respect to the parameter u_h. The normalized quantity is thus proportional to the frequency of the parameter u_h per unit volume of configuration space. This volume element is a function of u_h, e.g.,

$$\begin{aligned} &v(R_{OO}) = 4\pi R_{OO}^2 , \\ &v(\theta_H) = \sin(\theta_H) , \\ &v(\theta_{LP}) = \sin(\theta_{LP}) , \\ &v(\delta_D) = 1 . \end{aligned} \tag{4}$$

The relevant quantities for network analysis based on the work of Geiger *et al.*[8] are as follows: Let N denote the number of molecules considered and for a given configuration, let m_n be the number of H-bonded clusters consisting of n molecules. Let M the total number of clusters. Then the average cluster size, $\langle n \rangle$, will be given as

$$\langle n \rangle = N/M , \tag{5}$$

and the fluctuations in the cluster size, $\langle n_w \rangle$, is

$$\langle n_w \rangle = \langle n^2 \rangle / \langle n \rangle = \sum_{n=1}^{N} n^2 m_n / M . \tag{6}$$

A gel cluster is defined as a cluster with $n > 1$. The number of gel clusters is denoted by M_g, and the average gel-cluster size by $\langle n_g \rangle$. The number of unbound waters (clusters with $n = 1$) is denoted by N_u.

The results of the H-bond network analyses of molecular dynamics simulations of liquid water based on the ST2 potential showed that the key variable is the average number of H bonds per molecule $\bar{n}_{HB}$.[8] Expressing properties as a function of $\bar{n}_{HB}$ has the further advantage that it makes possible the comparison of different H-bond definitions. Furthermore, Geiger *et al.* have sought to eliminate the effect of the system size by normalizing all quantities by N.

TABLE I. Specifications of the Monte Carlo calculations analyzed.[a]

System	W–W potential	S–W potential	N	Length (K)	Boundary conditions	Temperature (°C)
$[H_2O]_l$	MCY	···	125	4400	sc	25
$[H_2O]_l$	ST2	···	216	4900	sc	10
$[H_2O]_l$	MCY	···	216	1500	fcc	37
$[H_2O]_l$	MCY	···	216	2200	fcc	50
$[CH_4]_{aq}$	MCY	HPF	125	500	sc	25
$[Li^+]_{aq}$	MCY	KPC	216	1000	fcc	25
$[Na^+]_{aq}$	MCY	KPC	216	1000	fcc	25
$[K^+]_{aq}$	MCY	KPC	216	850	fcc	25
$[F^-]_{aq}$	MCY	KPC	216	1000	fcc	25
$[Cl^-]_{aq}$	MCY	KPC	216	1000	fcc	25

[a](a) The length of the run is in the unit of 1000 steps; (b) sc stands for simple cubic and fcc strands for face-centered-cubic periodic boundary conditions; (c) MCY: Ref. 13, ST2: Ref. 15, HPF: Ref. 5, KPC: Ref. 30.

In addition to these quantities, we also computed the average fraction of bonds that can be removed without changing the sizes of the clusters, called loop-forming bonds $\langle x_l \rangle$:

$$x_l = (N_{HB} - N + M)/N_{HB} \ . \tag{7}$$

Here N_{HB} is the total number of H bonds in a given configuration. The magnitude of this quantity is directly related to the applicability of the polymerization theories of Flory[26] and Stockmayer,[27,28] where $x_l = 0$ is assumed. This quantity is closely related to the cyclomatic number in percolation theory.[29]

Extending the concept of H-bond QCDF's to aqueous solutions requires special considerations depending on the nature of the solute. For dilute aqueous solutions of ions, the solvent QCDF analysis was based only on water molecules outside the first solvation shell and inside the inscribed sphere tangent to the unit cell. This obviates making H-bond decisions about water molecules strongly bound to solute ions. This part of the system can be tentatively identified with the Frank and Wen B region. For $[CH_4]_{aq}$ the first solvation layer was examined separately in the analysis since it is expected from basic ideas about hydrophobic hydration to remain intrinsically part of the solvent H-bond network.

The effect of the solute on the extent of H bonding in network analysis is more difficult to assess since the properties to be examined are not local. As a result, the comparison of the network parameter distributions of the bulk system with a spherical shell of the corresponding solvated water would lead to misleading results. To circumvent this difficulty, network analyses of solutions were always performed on the complete solvent system with an additional assumption about the relation of the solute atom to the network. In the ionic solutions, the solute ion is always included in the net via interactions with the waters in the first solvation shell. In $[CH_4]_{aq}$, the solute atom is excluded due to its hydrophobic nature. These assumptions are seen to be consistent with those described in the preceding paragraph for the H-bond QCDF calculations. These constraints could bias the network analysis of ionic solutions toward more extended networks and the methane solution toward less extended networks, but these effects are expected to be small.

IV. CALCULATIONS

This analysis is based on Monte Carlo Metropolis computer simulations on water and dilute aqueous solutions using both the MCY[13] and the ST2[15] potentials for water–water interaction and *ab initio* quantum-mechanical potentials for the interaction of water and monatomic cations and anions (Li^+, Na^+, K^+, F^-, Cl^-),[30] and of water and methane.[5] The system size, length of the run, potential functions used, temperature, and the boundary conditions applied are summarized in Table I. The systems were studied at their experimental density, with the exception of the ST2 water, where $\rho = 1.000$ g/cm^3 has been used to remain consistent with previous calculations.

The computation of H-bonding QCDF's for liquid water is based on the 973–4400 K segment of the 25 °C MCY simulation and on the 2802–4962 K segment of the ST2 simulation. Convergence characteristics of Monte Carlo Metropolis simulation on MCY and ST2 water were described in detail in a previous paper.[4] The convergence indices in the MCY simulation were found to exhibit an oscillatory behavior with small amplitude (~0.2 kcal/mol in the energy) and very long period (~1500 K). The effect of this behavior was studied previously by considering averages over the "high" and "low" phases of the oscillations, denoted by segment A, B, and C, A and C having higher energy than B. As evidenced by the behavior of the radial distribution functions, the B segment was more structured in the icelike sense than A and C. This A, B, C segment notation is not to be confused with the solvent water A, B, C regions as described above. The magnitude of this effect in pure water can be considered as an error bound on calculated water perturbations, and QCDF differences must exceed these magnitudes to be considered statistically significant. These error bounds are likely to be more reliable than the technique based on block averages[31] since the oscillatory behavior implies a correlation between the blocks. The results on these individual segments are referred to subsequently for calibration of structuration

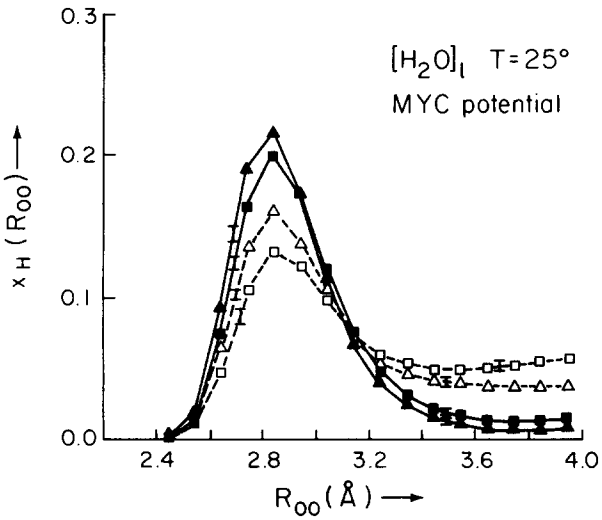

FIG. 2. QCDF's for the parameter R_{OO}, MCY water at 25 °C. ■: $x_H(R_{OO})$, strong H bond; ▲: $x_H(R_{OO})/v(R_{OO})$, strong H bond; □: $x_H(R_{OO})$, weak H bond; △: $x_H(R_{OO})/v(R_{OO})$, weak H bond.

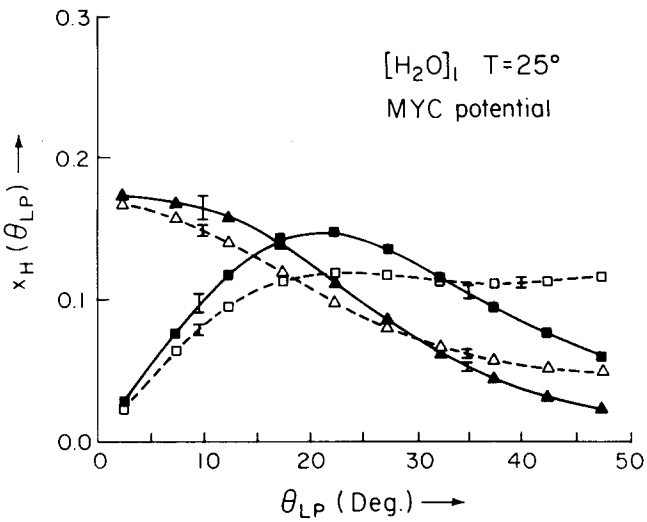

FIG. 4. QCDF's for the parameter θ_{LP}, MCY water at 25 °C. Symbols as in Fig. 2.

indices in the analyses of solvent structure in solutions.

The computation of the QCDF's has been performed by fully analyzing each $2N$th configuration. The minimal H-bond specification with $R_{max}=4.0$ Å was used, referred to hereafter as the "weak" H-bond definition. We also computed the QCDF's for the other H-bond definition, hereafter referred to as the "strong" H-bond case, corresponding to the cutoffs $R_{OO}=3.3$ Å, $\theta_H=45°$, $\theta_{LP}=45°$, and $\delta_D=90°$. The contributions from each configuration have been collected into the joint four-dimensional QCDF of the four H-bond parameters, represented over a finite, four-dimensional grid. The grid sizes used for the four parameters were 0.1 Å, 5°, 5°, and 10°, respectively. Integrating out (by simple summation) three of the four parameters gives the QCDF $x_H(u_h)$ for the remaining fourth.

In the network analysis of H bonding in liquid water the computation of the cluster distributions were based on the analysis of every 5000th configuration. By comparing the results from one MCY analysis (with $N=125$) where every 2000th configuration was analyzed, we concluded that the error introduced by the decreased number of configurations considered is about 1%.

It is also desirable to study the network analysis as a function of the H-bonding strength. The variation of the H-bond strength requires systematic variation at all cutoff values in the H-bond definition. In the present study the interoxygen distance, R_{OO}, was varied independently while the angular cutoffs c_h were simultaneously varied in such a way that

$$\int_0^{c_h} x_H(u_h)du_h = 0.3, 0.4, 0.5, \ldots, 1.0\,, \quad u_h=\theta_H, \theta_{LP}, \delta_D\,. \tag{8}$$

The values of c_h were obtained by integrating the joint

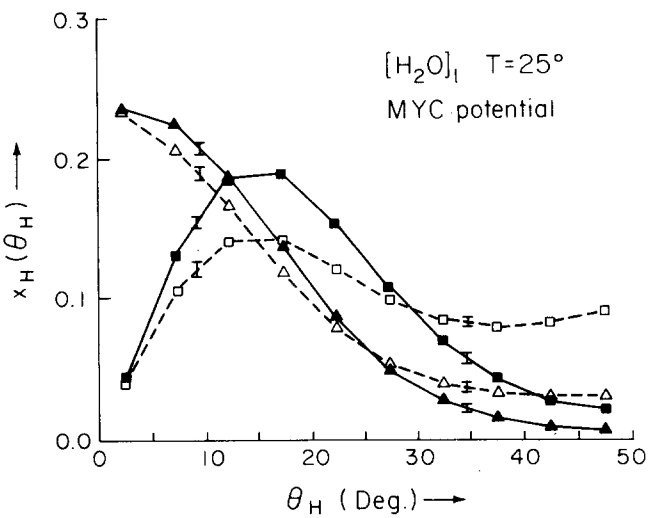

FIG. 3. QCDF's for the parameter θ_H, MCY water at 25 °C. Symbols as in Fig. 2.

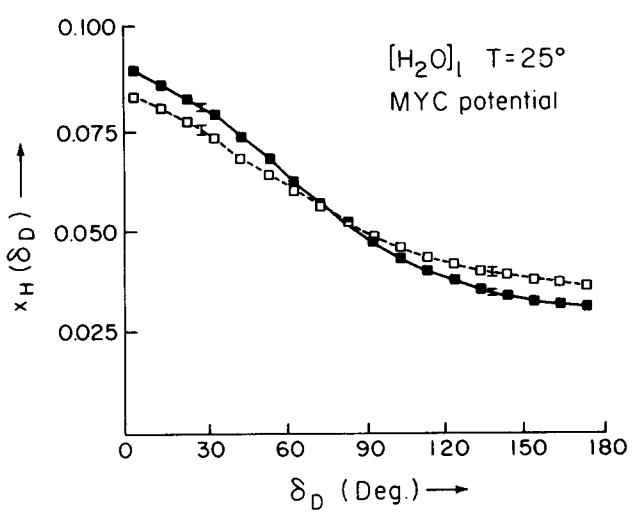

FIG. 5. QCDF's for the parameter δ_D, MCY water at 25 °C. Symbols as in Fig. 2.

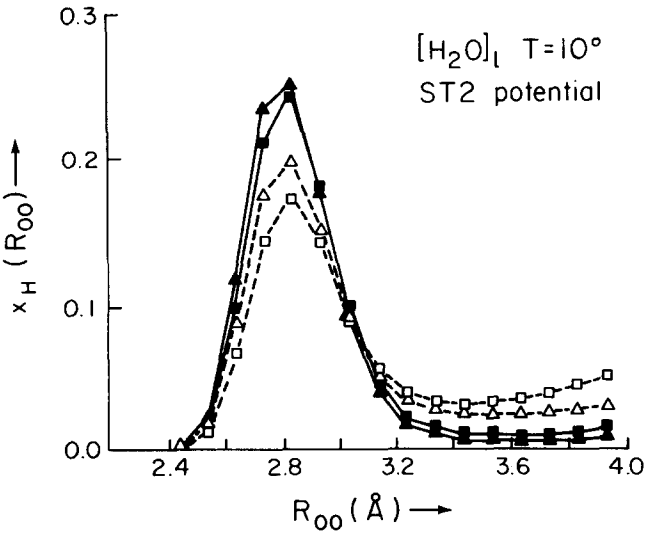

FIG. 6. QCDF's for the parameter R_{OO}, ST2 water at 10 °C. Symbols as in Fig. 2.

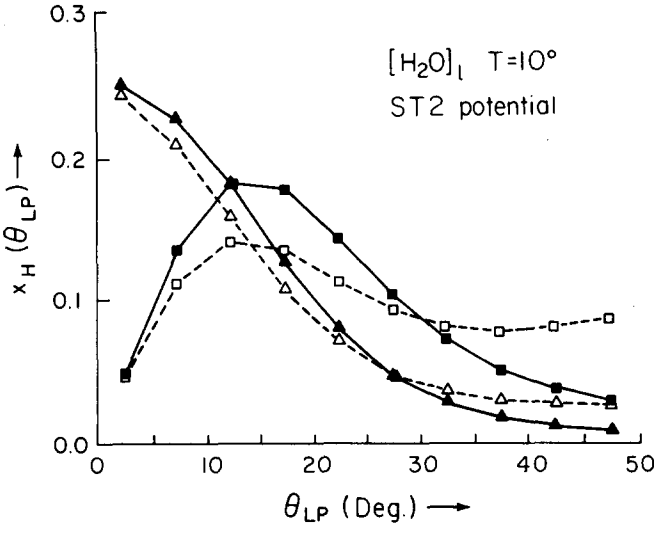

FIG. 8. QCDF's for the parameter θ_{LP}, ST2 water at 10 °C. Symbols as in Fig. 2.

four-dimensional QCDF obtained previously. Note that this determination of the angular cutoffs is based on ensemble average quantities and thus are very slightly temperature dependent.

V. RESULTS

The H-bond QCDF's computed from simulation results on MCY water are shown in Figs. 2–5 and for the ST2 water at 10 °C in Figs. 6–9. Each figure contains $x_H(u_h)$ and $x_H(u_h)/v(u_h)$ for both the strong and the weak H-bond definitions. The values of $x_H(u_h)$ and $x_H(u_h)/v(u_h)$ at their respective maxima are collected in Table II for the weak H-bond case and in Table III for the strong H-bond case. Tables II and III also contain the H-bond QCDF values for segments B and C of the MCY run. Error bars are displayed for representative points of Figs. 2–5, based on the curves obtained (but not shown here) for segments B and C. We also computed the joint H-bonding QCDF's of the H-bond parameter pairs. These distributions are not displayed here since, after inspection, we found that their inclusion introduces no new information beyond that emerging from the one-dimensional QCDF's. The QCDF values for solvent water at the maxima of the pure water QCDF's are also shown in Tables II and III for the weak and strong H-bond definitions together with the results from the liquid water simulation based on the MCY potential performed at 37 and 50 °C.

The network analysis on pure water involved calculation of $\langle n\rangle$, $\langle n\rangle_g$, $\langle M\rangle$, $\langle M_g\rangle$, $\langle n_w\rangle$, $\langle N_u\rangle$ for the MCY water at 25 and 37 °C using 125 and 216 particle systems and for the ST2 water at 10 °C using 216 molecules. The average number of H bonds per molecule, $\bar{n}_{HB}$, corresponding to the different cutoff values is given in Tables IV–VI for the 25 °C MCY, 37 °C MCY, and 10 °C ST2 waters, respectively. Since the H-bond strength was varied by changing two independent cutoff values, the same value of $\bar{n}_{HB}$ can be obtained from different cutoff

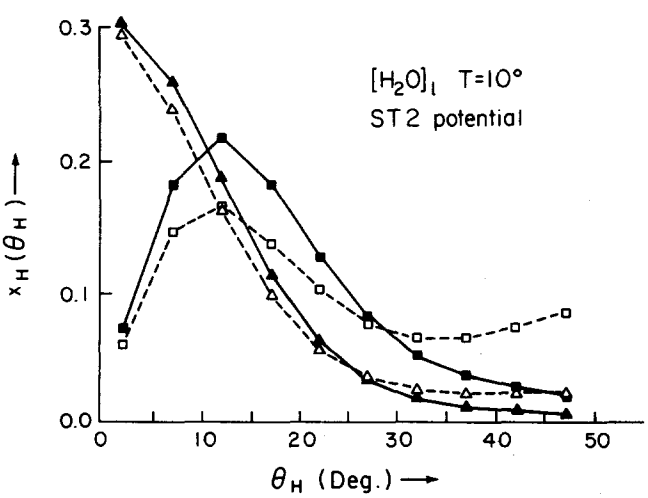

FIG. 7. QCDF's for the parameter θ_H, ST2 water at 10 °C. Symbols as in Fig. 2.

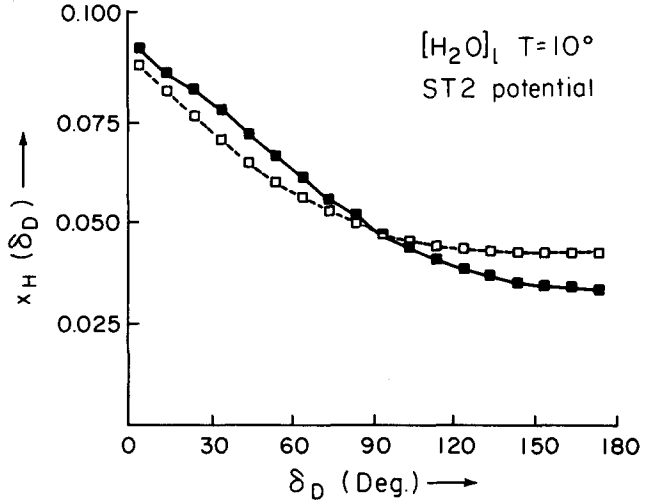

FIG. 9. QCDF's for the parameter δ_D, ST2 water at 10 °C. Symbols as in Fig. 2.

TABLE II. QCDF values at selected points using the weak H-bond definition.[a]

QCDF: Position	$x_H^n(R_{OO})$ 2.85 Å	$x_H(\theta_H)$ 17.5°	$x_H^n(\theta_H)$ 2.5°	$x_H(\theta_{LP})$ 22.5°	$x_H^n(\theta_{LP})$ 2.5°	$x_H(\delta_D)$ 2.5°
System						
$[H_2O]_I$, 25°	0.159	0.144	0.232	0.121	0.168	0.0838
$[H_2O]_I$, *B*	0.161	0.145	0.235	0.122	0.151	0.0844
$[H_2O]_I$, *C*	0.156	0.143	0.228	0.119	0.164	0.0824
$[H_2O]_I$, 37°	0.159	0.144	0.232	0.121	0.168	0.0838
$[H_2O]_I$, 50°	0.150↓	0.119↓	0.212↓	0.094↓	0.144↓	0.0804↓
$[H_2O]_I$, ST2	0.174	0.168	0.300	0.145	0.251	0.0887
$[Li^+]_{aq}$	0.154	0.139	0.231	0.121	0.159	0.0814↓
$[Na^+]_{aq}$	0.158	0.141↓	0.230	0.119	0.166↓	0.0840
$[Na^+]_{aq}$, S2	0.164↑	0.136↓	0.117↓	0.122↑	0.178↓	0.0869↑
$[K^+]_{aq}$	0.157	0.141↓	0.236↑	0.119	0.168↓	0.0899↑
$[F^-]_{aq}$	0.153↓	0.139↓	0.221↓	0.118	0.158	0.0823↓
$[Cl^-]_{aq}$	0.157	0.142↓	0.229	0.120	0.161	0.0836
$[CH_4]_{aq}$, S1	0.162↑	0.154↑	0.242↑	0.122	0.181↓	0.0901
$[CH_4]_{aq}$	0.164↑	0.145	0.244↑	0.122	0.166↓	0.0848↑

[a](a) The system labeled with ST2 used the ST2 potential for water–water interactions, all other systems used the MCY potential; (b) The labels *B* and *C* refer to the more and less structured segment of the 25° Monte Carlo run; (c) S1 and S2 refers to results involving only water molecules in the first and second solvation shell, respectively; (d) The maxima of $x_H(\theta_H)$ and $x_H(\theta_{LP})$ are at 12.5° for the ST2 water; (e) The signs ↓ and ↑ after a number mark the values that deviated in the direction of lower and higher structure, respectively; (f) The superscript n represents the normalized QCDF $x_H(u_h)/v(u_h)$.

combinations. The results are collected in Figs. 10–12. Figures 10 and 11 also contain data obtained from Figs. 6 and 7 of Ref. 8.

The values obtained for $\bar{n}_{HB}$ using different H-bond definitions can also serve as a basis for comparison of the different H-bond definitions used. We obtained $\bar{n}_{HB} = 2.10$ and 5.22 with the strong and weak H bonds for the MCY water at 25 °C, respectively, and 2.36 and 5.21 on the ST2 water at 10 °C, respectively. In terms of ST2 energy cutoffs this is equivalent to −4.1 and −1.4 kcal/mol for the MCY water at 25 °C and to −3.8 and −1.4 kcal/mol for the ST2 water at 10 °C. The temperature invariant point in the ST2 pair energy distribution suggested a "natural" cutoff of −4.0 kcal/mol, yielding $\bar{n}_{HB} = 2.2$, essentially coinciding with our strong H-bond definition. Calculations by Jorgensen[18] with another quantum-mechanical potential[17] led to the choice of an

TABLE III. QCDF values at selected points using the strong H-bond definition.[a]

QCDF Position	$x_H^n(R_{OO})$ 2.85 Å	$x_H(\theta_H)$ 17.5°	$x_H^n(\theta_H)$ 2.5°	$x_H(\theta_{LP})$ 22.5°	$x_H^n(\theta_{LP})$ 2.5°	$x_H(\delta_D)$ 2.5°
System						
$[H_2O]_I$, 25°	0.216	0.192	0.237	0.148	0.171	0.0904
$[H_2O]_I$, *B*	0.218	0.194	0.238	0.149	0.174	0.0901
$[H_2O]_I$, *C*	0.214	0.190	0.233	0.147	0.165	0.0908
$[H_2O]_I$, 37°	0.216	0.192	0.237	0.148	0.170	0.0904
$[H_2O]_I$, 50°	0.205↓	0.178↓	0.234↓	0.133↓	0.162↓	0.0879
$[H_2O]_I$, ST2	0.252	0.219	0.302	0.184	0.253	0.0929
$[Li^+]_{aq}$	0.214	0.186↓	0.238	0.147	0.165	0.0917
$[Na^+]_{aq}$	0.218	0.191	0.237	0.148	0.169	0.0928
$[Na^+]_{aq}$, S2	0.226↑	0.183↓	0.208↓	0.152↑	0.186↓	0.0961
$[K^+]_{aq}$	0.216	0.187↓	0.242↑	0.148	0.171	0.0920
$[F^-]_{aq}$	0.211↓	0.190↓	0.228↓	0.146↓	0.162↓	0.0923
$[Cl^-]_{aq}$	0.216	0.191	0.236	0.148	0.166	0.0920
$[CH_4]_{aq}$, S1	0.218	0.201↑	0.245↑	0.150↑	0.178↑	0.0952
$[CH_4]_{aq}$	0.220↑	0.192↑	0.241↑	0.152↑	0.164↓	0.0913

[a](a) The system labeled with ST2 used the ST2 potential for water–water interactions, all other systems used the MCY potential; (b) The labels *B* and *C* refer to the more and less structured segment of the 25° Monte Carlo run; (c) S1 and S2 refers to results involving only water molecules in the first and second solvation shell, respectively; (d) The maxima of $x_H(\theta_H)$ and $x_H(\theta_{LP})$ are at 12.5° for the ST2 water; (e) The signs ↓ and ↑ after a number mark the values that deviated in the direction of lower and higher structure, respectively; (f) The superscript n represents the normalized QCDF $x_H(u_h)/v(u_h)$.

TABLE IV. Average number of H bonds per molecule for the different cutoff values on MCY water, $T = 25\,^{\circ}C$.[a]

	Combined angular cutoff						
R_{max}	0.3	0.4	0.5	0.6	0.7	0.8	0.9
2.8				0.216	0.350	0.522	0.743
2.9					0.645	0.961	1.35
3.0				0.567	0.919	1.37	1.91
3.1			0.407	0.718	1.15	1.70	2.34
3.2	0.106	0.257	0.455	0.841	1.36	1.96	2.73
3.3	0.112	0.276	0.550	0.960	1.50	2.19	3.00
3.4	0.128	0.314	0.619	1.10	1.66	2.39	3.25
3.6	0.163	0.399	0.779	1.31	1.98	2.77	
3.8	0.206	0.492	0.944	1.56	2.29	3.14	
4.0	0.258	0.603	1.14	1.80	2.57		

[a](a) R_{max} is defined in Eq. (1); (b) The combined angular cutoff is defined in Eq. (8).

energy cutoff -2.25 kcal/mol (to coincide with the minimum of the pair-energy distribution of that potential), resulting in $\bar{n}_{HB} = 3.4$ for that study. Thus the cutoff used by Jorgensen is approximately equivalent to a -2.6 kcal/mol ST2 energy cutoff.

The $\bar{n}_{HB}$ values for the strong H-bond definition are compared with the average coordination number corresponding to the same radial cutoff in Table VII. The average coordination number indicates that there are four nearest neighbors but only 50% of the near-neighbor pairs are strongly H bonded with this definition. For the weak H-bond definition this ratio increases to 78% for the MCY water and 82% for the ST2 water. It should be pointed out, however, that the relatively low number obtained for $\bar{n}_{HB}$ still permits the formation of extended H-bonded networks. As can be seen on Fig. 10, the mole fraction of unbound water molecules is less than 0.05 if $\bar{n}_{HB}$ is greater than 2.0, and the number of water monomers present is thus negligibly small.

The network analysis on solvating water showed that the effect of the solute on the network parameter distributions is rather small. Table VII contains the $\bar{n}_{HB}$ values for the various solvated waters. Note, that these values refer to all waters in the system. Comparison of the network parameters obtained for the solvating waters with the value of the network parameter distribution functions for pure water at the $\bar{n}_{HB}$ value corresponding to the solute in question revealed no statistically significant change.

TABLE V. Average number of H bonds per molecule for the different cutoff values of ST2 water, $T = 10\,^{\circ}C$.[a]

	Combined angular cutoff						
R_{max}	0.3	0.4	0.5	0.6	0.7	0.8	0.9
3.0	0.104	0.249	0.493	0.854	1.33	1.91	2.55
3.2	0.145	0.344	0.645	1.13	1.74	2.45	3.23
3.3	0.162	0.377	0.737	1.23	1.87	2.61	3.42
3.6	0.203	0.481	0.925	1.52	2.23	2.98	3.82
4.0	0.281	0.661	1.24	1.95	2.68	3.52	4.34

[a](a) R_{max} is defined in Eq. (1); (b) The combined angular cutoff is defined in Eq. (8).

TABLE VI. Average number of H bonds per molecule for the different cutoff values on MCY water, $T = 37\,^{\circ}C$.[a]

	Combined angular cutoff						
R_{max}	0.3	0.4	0.5	0.6	0.7	0.8	0.9
3.0	0.065	0.161	0.324	0.570	0.913	1.36	1.89
3.2	0.099	0.245	0.491	0.840	1.32	1.96	2.70
3.3	0.115	0.250	0.553	0.962	1.50	2.18	2.99
4.0	0.063	0.607	1.12	1.78	2.55	3.47	4.33

[a](a) R_{max} is defined in Eq. (1); (b) The combined angular cutoff is defined in Eq. (8).

VI. DISCUSSION

This section deals with the following topics: (a) the interpretation of H-bond QCDF's for the MCY and ST2 description of liquid water; (b) the temperature dependence of the H-bond QCDF's for liquid water; (c) the effect of ionic and hydrophobic solutes on the solvent water H-bond QCDF's; (d) the comparison of the network analysis results for the various descriptions of liquid water and for the energetic and geometric definition of H bond.

Consider first the MCY water H-bonding QCDF's. The quantities $x_H(R_{OO})$ and $x_H(R_{OO})/(4\pi R_{OO}^2)$ for both the strong and the weak H-bond definitions in Fig. 2 show a strong peak coincident with the first peak of the calculated center-of-mass radial distribution function $g(R)$.

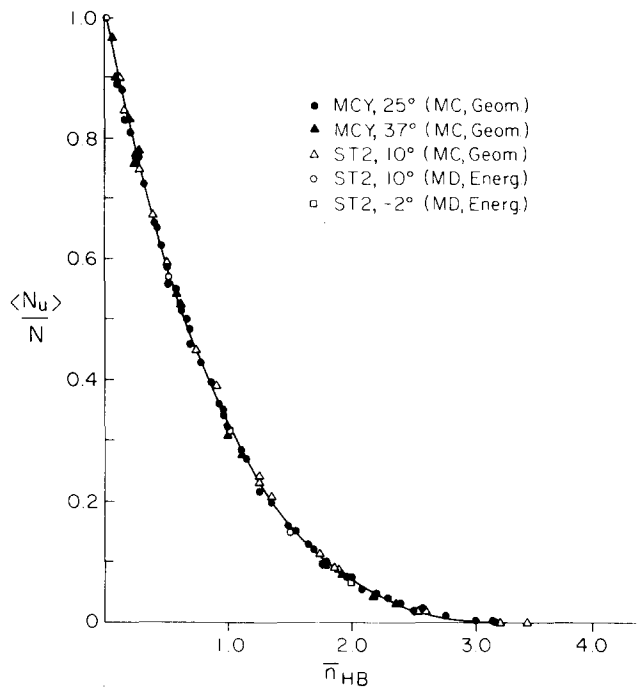

FIG. 10. Average number of unbound molecules, $\langle N_u \rangle / N$, as a function of the average number of H bonds per molecule, $\bar{n}_{HB}$, for various systems. ●: MCY water, $T = 25\,^{\circ}C$, $N = 125$, geometric criterion, Monte Carlo run; ▲: MCY water, $T = 37\,^{\circ}C$, $N = 216$, geometric criterion, Monte Carlo run; ○: ST2 water, $T = 10\,^{\circ}C$, $N = 216$, geometric criterion, Monte Carlo run; △: ST2 water, $T = 10\,^{\circ}C$, $N = 216$, energetic criterion, molecular dynamics run; □: ST2 water, $T = -1\,^{\circ}C$, $N = 1728$, energetic critierion, molecular dynamics run.

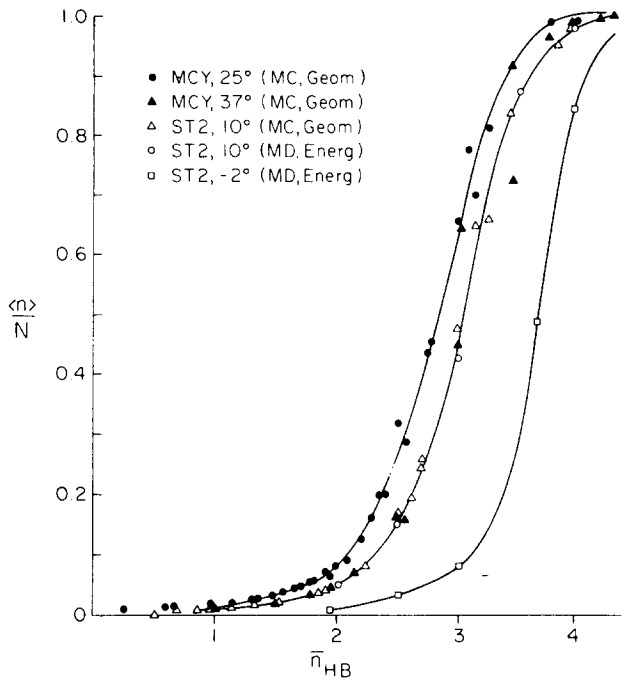

FIG. 11. Average cluster size, $\langle n\rangle/N$, as a function of the average number of H bonds per molecule, $\bar{n}_{HB}$, for various systems. Symbols as in Fig. 10.

This confirms as expected the dominant role of intermolecular H bonding in determining the structure of the system. In the angular QCDF's, $x_H(\theta_H)$ has a peak at $\theta_H = 17.5°$ and $x_H(\theta_{LP})$ has a peak at $\theta_{LP} = 22.5°$ for both the strong and the weak H-bond definitions. The shapes of the two curves are quite similar. This result indicates that the essential structural feature in the statistical state of the system is bent H bonds. At first sight this appears to be in contradiction to the known preference of the water dimer to form linear H bonds, but consideration of the normalized QCDF's $x_H(\theta_H)/\sin(\theta_H)$ and $x_H(\theta_{LP})/\sin(\theta_{LP})$ leads to a simple explanation. Both normalized QCDF's peak at 0°. This shows that if one considers the probability of observing an angle θ_H or θ_{LP} per unit volume of configuration space then the linear geometry will be assigned the highest probability. Thus the preference for bent H bonds in liquid water is a consequence of the structure of the configuration space, i.e., of statistical as well as energetic effects. The quantity $x_H(\delta_D)$ peaks at $\delta_D = 0°$ and shows a nearly linear behavior with a rather small slope. This implies that the description of H bonding is essentially insensitive to variations in δ_D.

TABLE VII. Average number of H bonds per molecule and the corresponding coordination numbers for the strong H-bond definitions.

System	$\bar{n}_{HB}$	$\bar{K}$
$[H_2O]_I$, 25°	2.14	4.29
$[H_2O]_I$, *B*	2.12	4.25
$[H_2O]_I$, *C*	2.10	4.25
$[H_2O]_I$, 37°	2.03	4.24
$[H_2O]_I$, 50°	1.95	4.20
$[H_2O]_I$, ST2	2.36	4.75
$[Li^+]_{aq}$	2.05	4.35
$[Na^+]_{aq}$	2.14	4.23
$[Na^+]_{aq}$	2.08	4.24
$[F^-]_{aq}$	2.10	4.30
$[Cl^-]_{aq}$	2.10	4.27
$[CH_4]_{aq}$	2.10	4.54

In the H-bond analysis of the ST2 water (Figs. 6–9) we see that all QCDF's have higher and narrower peaks for ST2 water than the corresponding MCY water QCDF's. This is a quantitative indication of the extent that the ST2 water is more structured in the icelike sense than the MCY water. Furthermore, the difference between $x_H(\theta_H)$ and $x_H(\theta_{LP})$ is much less for the ST2 water than for the MCY water, indicating that the degree of symmetry between hydrogens and lone pairs is higher in the ST2 than in the MCY water.

Comparison of the H-bond QCDF results based on both the strong and weak H-bond definition shows that the qualitative picture is essentially identical for both cases and independent of the potential function. The more restricted nature of the strong H bond causes a general narrowing of the QCDF's. This result implies that any H-bond definition that lies in the range spanned by our weak and strong H-bond definitions would give the same qualitative structural picture of the system and the QCDF's from intermediate H-bond definitions can be interpolated from the ones obtained here.

Certain experimental estimates of the average H-bond angle are available for comparison. Sceats and Rice in their work on the random network model[21,22] obtained values for the mean square average of the H-bond angle, $\langle\theta_H^2\rangle^{1/2}$, from IR data by assuming that $\langle\theta_H^2\rangle^{1/2}$ and $\langle\theta_{LP}^2\rangle^{1/2}$ have identical distribution. The values obtained range from 18° to 21° depending on the temperature and the particulars of the calculation. If $\langle\theta_H^2\rangle^{1/2}$ and $\langle\theta_{LP}^2\rangle^{1/2}$ are approximated by the respective locations of the peaks of $x_H(\theta_H^2)$ and $x_H(\theta_{LP}^2)$, our results on the MCY water are in

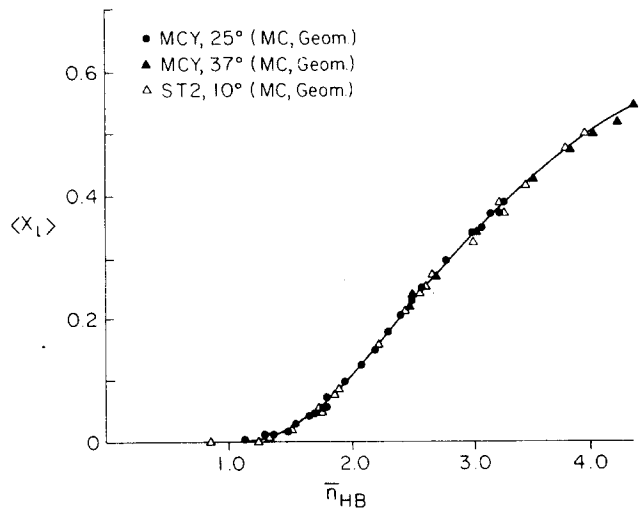

FIG. 12. Average fraction of loop-forming bonds, $\langle x_l\rangle$, as a function of the average number of H bonds per molecule, $\bar{n}_{HB}$, for various systems. Symbols as in Fig. 10.

good accord with their interpretation of the experimental data. Furthermore, the difference between $\langle\theta_H^2\rangle^{1/2}$ and $\langle\theta_{LP}^2\rangle^{1/2}$ is found to be small but significant. This finding could form a basis of small refinement of the Sceats–Rice random network model. For the ST2 potential the predicted values of $\langle\theta_H^2\rangle^{1/2}$ and $\langle\theta_{LP}^2\rangle^{1/2}$ are both 12.5°, implying that the ST2 potential predicts excessively high librational frequencies. Overall, however, all these computer simulation results strongly support the validity of viewing liquid water structure in terms of a random network model of water molecules interacting mainly via bent H bonds.

The variations in the H-bond structure caused by a solute or a change in temperature were considered by comparing the H-bond QCDF's of the bulk water with the QCDF's of the solvating water or water at different temperatures. As discussed earlier, the MCY calculation was previously divided into segments that exhibited small but clearly discernable differences in behavior.[4] The changes in energy, radial distribution function, and coordination number distribution were consistently displaying higher structuration in one segment than in the other two, as evidenced for example by the height and shape of the first peak in the calculated $g(R)$. Thus, changes in the H-bonding QCDF's can be qualified as indicative of increased or decreased structuration by computing them over these same segments of the MCY run. The values (given in Tables II and III) show that the changes closely follow intuitive expectations regarding structure, i.e., increased icelike character is evidenced by increased peak height and narrowed peak shapes. The changes using the weak and strong H-bond definitions are in the same direction with two exceptions: (a) $x_H(\delta_D)$ with the strong hydrogen-bond definition decreases slightly with increased structuration where the difference is very small, and (b) $x_H(\theta_{LP})/\sin(\theta_{LP})$, where the peak at 0° with the weak definition is rather shallow, making the result plausible. In order to emphasize the structuration or destructuration character of the solutes on the solvent or the change in temperature, in Tables II and III the values that significantly changed in the direction of more structure (in the above defined sense) were marked with a sign "↑" and the values that changed in the direction of less structure were marked with a sign "↓". When a QCDF value lay between the values determined for segments B and C, the change may not be statistically significant.

The H-bond results from the Monte Carlo simulation on MCY water performed at 37°C are similar to the 25°C results, the values falling between the corresponding B and C segment values in all cases. The 12°C difference did not effect statistically significant changes in the H-bond distribution functions. The temperature effect on the radial distribution function and on the average number of H bonds is more noticeable, and as expected is in the direction of the loss of structure. The results at 50°C show a statistically significant consistent loss in the H-bond structure of the fluid.

The results on the ionic solutions show that only the two smallest ions, Li^+ and F^-, exhibit a consistent behavior, in the direction of the destructuration. Cl^- has little net effect at all. The effect of Na^+ and K^+ is ambiguous, i.e., some indices change in the structure making directions while others in the structure breaking directions. The study of the second shell around Na^+ shows a similar picture: while the deviations are larger than for the calculation involving more water molecules, the various H-bond indices give conflicting results with respect to structuration. The solvent changes in the methane solution are generally in the direction of increased structure. The general difficulty here is that the perturbations on solvent structure are very small, and significant results using systems of O(100) particles and realizations of presently tractable lengths, O(1000 K), are difficult to obtain.

An explanation of the significant changes observed follows from a detailed consideration of how solvent structuration effects depend upon the type of solute in the solution. Ionic solutes will invariably introduce electrostrictive structure in the solvent A region, due to the strong ion–water binding interactions. Water in the B region in this system must interface two structurally incompatible structures, the electrostricted A region and the H-bonded bulk water region. The B region is thus necessarily less electrostrictively structured than the A region and also has less icelike character than bulk water. The latter accounts for the observed trend in the calculated results in Tables II and III for the aqueous hydration of ions. The above points are particularly well illustrated by the results on the $[Li^+]_{aq}$ and $[F^-]_{aq}$ systems. Data in Tables II and III show that the B region exhibits the greatest loss of structuration in the icelike sense for these ions, in agreement with earlier results on the B-region water–water $g(R)$ and $x_C(K)$. At the same time, the greatest electrostrictive structuration in the A region occurs with just these ions, as can be inferred from the size and shape of the first peak of the ion–water $g(R)$ and of the near-neighbor ion–water dipole correlation function, $x_D(\theta)$.[6]

The trend towards increased structure for the region of solvent examined in $[CH_4]_{aq}$ can be explained from similar considerations on apolar solutes. In hydrophobic hydration, the solute induces a clathratelike cage structure in the solvent A region, a structure with increased icelike character and stronger intermolecular H bonds than in bulk water. This effect was studied in detail in a previous paper.[5] The solvent B region in this system shows increased icelike character as it interfaces the highly structured water clathrate with bulk water. This explains the observed trend in the calculated results on the aqueous hydration of CH_4.

It is desirable to formulate some overall index of structuration for aqueous solutions and to account for observed classifications of solutes as structure makers or structure breakers in terms of molecular distribution functions. However, here different types of structurations would have to be quantitatively weighted with no clear theoretical basis on which to proceed. Numerical limitations follow from the fact that the solvent perturbations are so small, as seen from the results in Tables II and III. The best direct approach to the problem of overall structuration would be to calculate the

entropy of the system from computer simulation. Here the ill-conditioned nature of the configurational integrand for entropy makes numerical calculations along standard lines problematic.[3,32] The calculated heat capacity is a possible index for consideration, but it is also expected to be a very slowly converging quantity in computer simulation of solutions.[4,33] A general account of structure making and structure breaking in aqueous solutions is thus a challenging area for future research.

The network analysis of Geiger *et al.* found that the normalized functions $\langle M\rangle/N$, $\langle n_w\rangle/N$, $\langle M_g\rangle/N$, $\langle N_u\rangle/N$ are remarkably independent of the system size and temperature while the quantities $\langle n\rangle/N$ and $\langle n\rangle_g/N$ exhibit significant change with variation in the system size and/or the temperature. The results of our studies are generally consistent with these findings, as demonstrated with Figs. 10 and 11. In particular, the quantities found invariant to the system size and the temperature are also invariant to the replacement of the energetic H-bond definition with our geometric H-bond definition. The curves of $\langle n\rangle/N$ reveal that variation in the system size induces changes in the curve while small changes in the temperature and in the type of H-bond definition leave $\langle n\rangle/N$ mostly unchanged, although there is some "scatter" in the region $\bar{n}_{HB}\sim 3-4$. This scatter is due to the fact that the same $\bar{n}_{HB}$ can be obtained in this range from very different cutoff combinations. Similar behavior was found for $\langle n\rangle_g/N$ (not shown here).

The average fraction of loop-forming bonds, $\langle x_l\rangle$, is also found to be independent of system size, temperature, and H-bond definition used. It becomes significantly different from zero only at the beginning of the percolation threshold, $\bar{n}_{HB}\sim 1.3$. This implies that the Flory–Stockmayer model is fully applicable for systems under the percolation threshold but would become increasingly inaccurate beyond this point.

The quantity $\langle x_l\rangle$ also gives an indication about the abundance of loops. Data from Figs. 10 and 11 imply that for the ST2 water at $\langle x_l\rangle = 0.1$ most clusters will contain one loop, at $\langle x_l\rangle = 0.2$ most clusters will contain ~ 5 loops, and at $\langle x_l\rangle = 0.3$ most clusters will contain ~ 18 loops. According to the results of Rahman and Stillinger on the distribution of H-bonded loops,[14] the most frequently occurring loops have 5–10 members. Using an average value of 8 we can conclude that at $\langle x_l\rangle < 0.2$ most H bonds are members of one loop, while at $\langle x_l\rangle > 0.3$ most H bonds are members of more than one loop. This arguments shows that loops are a prominent features of the H-bonded networks in water.

ACKNOWLEDGMENTS

This research was supported by NIH Grant # 5-R01-GM-24914 and a CUNY Faculty Research Award. Dr. S. Swaminathan contributed actively to this project at an early stage and his participation is gratefully acknowledged. We acknowledge also useful discussions with Dr. P. K. Mehrotra, Dr. F. T. Marchese, and Professor W. L. Jorgensen, who kindly supplied a preprint on his own H-bond analysis of simulation results.

[1] *Computer Modelling of Matter*, ACS Monograph series, edited by P. G. Lykos (American Chemical Society, Washington, D. C., 1978).
[2] S. Swaminathan and D. L. Beveridge, J. Am. Chem. Soc. 99, 8392 (1977).
[3] M. Mezei, S. Swaminathan, and D. L. Beveridge, J. Am. Chem. Soc. 100, 3255 (1978).
[4] M. Mezei, S. Swaminathan, and D. L. Beveridge, J. Chem. Phys. 71, 3366 (1979).
[5] S. Swaminathan, S. W. Harrison, and D. L. Beveridge, J. Am. Chem. Soc. 100, 5705 (1978); S. Swaminathan and D. L. Beveridge, J. Am. Chem. Soc. 101, 5832 (1979).
[6] M. Mezei and D. L. Beveridge J. Chem. Phys. (submitted for publication).
[7] A. Ben-Naim, *Water and Aqueous Solutions* (Plenum, New York, 1974).
[8] A. Geiger, F. H. Stillinger, and A. Rahman, J. Chem. Phys. 70, 4185 (1979).
[9] P. A. Kollman and L. C. Allen, J. Chem. Phys. 51, 3286 (1969); L. C. Allen, J. Am. Chem. Soc. 97, 6921 (1975).
[10] J. Del Bene and J. A. Pople, J. Chem. Phys. 52, 4858 (1970).
[11] D. Hankins, J. W. Moskowitz, and F. H. Stillinger, J. Chem. Phys. 53, 4544 (1970); 59, 995E (1973).
[12] G. F. H. Diercksen, Theor. Chim. Acta 21, 335 (1971).
[13] O. Matsuoka, E. Clementi, and M. Yoshimine, J. Chem. Phys. 64, 1351 (1976).
[14] A. Rahman and F. H. Stillinger, J. Am. Chem. Soc. 95, 7943 (1973).
[15] F. H. Stillinger and A. Rahman, J. Chem. Phys. 60, 1545 (1974).
[16] J. C. Owicki and H. A. Scheraga, J. Am. Chem. Soc. 99, 7403 (1977).
[17] W. L. Jorgensen, J. Am. Chem. Soc. 101, 2011 (1979).
[18] W. L. Jorgensen, J. Am. Chem. Soc. 101, 2016 (1979).
[19] W. L. Jorgensen, Chem. Phys. Lett. 70, 526 (1980).
[20] J. A. Pople, Proc. R. Soc. London Ser. A 205, 163 (1951).
[21] M. G. Sceats and S. A. Rice, J. Chem. Phys. 72, 3237 (1980).
[22] M. G. Sceats and S. A. Rice, J. Chem. Phys. 72, 3248 (1980); 72, 3260 (1980).
[23] W. L. Jorgensen, J. Am. Chem. Soc. 100, 7824 (1978).
[24] A. Holzer and M. F. Emerson, J. Phys. Chem. 73, 26 (1969).
[25] H. S. Frank and W. Y. Wen, Discuss. Faraday Soc. 24, 133 (1957).
[26] P. J. Flory, J. Am. Chem. Soc. 63, 3086 (1941); 63, 3091 (1941); 63, 3096 (1941).
[27] W. H. Stockmayer, J. Chem. Phys. 11, 45 (1943).
[28] C. Cohen, J. H. Gibbs, and P. D. Fleming III, J. Chem. Phys. 59, 5511 (1973).
[29] D. Stauffer, Phys. Rep. 54, 1 (1979).
[30] H. Kistenmacher, H. Popkie, and E. Clementi, J. Chem. Phys. 59, 5842 (1973).
[31] W. W. Wood, in *Physics of Simple Liquids*, edited by H. N. V. Temperley, F. S. Rowlinson, and G. S. Rushbrooke (North-Holland, Amsterdam, 1968).
[32] J. P. Valleau and G. M. Torrie, *Statistical Mechanics*, Part A, edited by B. J. Berne (Plenum, New York, 1977), p. 169.
[33] (a) C. S. Pangali, M. Rao, and B. J. Berne, Chem. Phys. Lett. 55, 413 (1979); (b) M. Rao, C. S. Pangali, and B. J. Berne, Mol. Phys. 37, 1779 (1979).